UCRL-JC-125875
PREPRINT

Superplastic Forming Using NIKE3D

M. Puso

This paper was prepared for submittal to the
Symposium of Engineering Mechanics in Manufacturing Processes and Materials
Processing for Joint ASME, ASCE, & SES
Evanston, Illinois
June 29-July 3, 1997

December 4, 1996

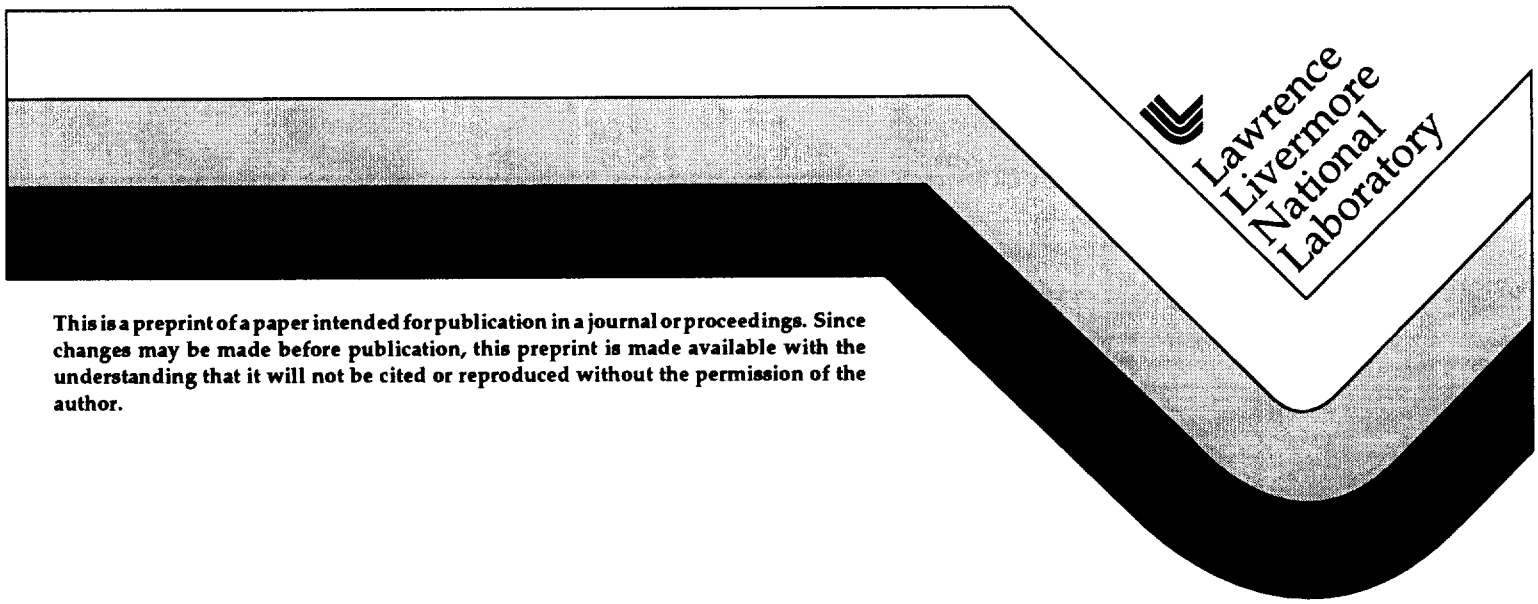

Superplastic Forming Using NIKE3D

Michael Puso

Methods Development Group L-125
Lawrence Livermore National Laboratory
Livermore, CA 94551

This paper was prepared for submittal to the Symposium of Engineering Mechanics in Manufacturing Processes and Materials Processing for the Joint ASME, ASCE, and SES Summer Meeting, June 29-July 3 1997, Evanston, Illinois

Abstract

The superplastic forming process requires careful control of strain rates in order to avoid strain localizations. A load scheduler was developed and implemented into the nonlinear finite element code NIKE3D to provide strain rate control during forming simulation and process schedule output. Often the sheets being formed in SPF are very thin such that less expensive membrane elements can be used as opposed to shell elements. A large strain membrane element was implemented into NIKE3D to assist in SPF process modeling.

This work was performed under the auspices of the U.S. Department of Energy by Lawrence Livermore National Laboratory under contract No. W-7405-Eng-48.

INTRODUCTION

Superplasticity is a term used for the deformation of certain metals under conditions which lead to unusually high elongations (hundreds of thousands of percent) without necking, tearing or other strain localization effects that normally occur with conventional materials subjected to large strains. For example, certain aluminum and titanium alloys are superplastic at temperatures of about half their melting point when being deformed at strain rates between 10^{-3} to 10^{-5} per second. Superplastic forming (or SPF) is the process in which bulk or sheet metal components are formed superplastically. Currently SPF is used for near-net-shape manufacturing of components for the automotive, aerospace and other industries. The superplastic behavior of materials throughout the forming operation enables complex parts to be manufactured in fewer stages with minimum waste. Therefore SPF can result in considerable cost savings when manufacturing a large number of complex parts or a moderate number of parts consisting of expensive or hazardous materials.

Superplasticity in production must be carefully controlled because there is a small range of strain rate and temperature for best formability without strain localization. Therefore the external loading applied (pressures, displacements, etc.) must be specified to meet these constraints. Typically this loading curve (i.e. pressure vs. time for blow forming) is the analyst's or designer's best estimate based on experience. This estimate may or may not produce the optimum strain rates necessary for superplastic forming to occur. To eliminate the necessity of a user input loading, a load scheduler was added to NIKE3D (Maker, 1995) to provide process control. The analyst simply inputs the desired strain rate thresholds as opposed to the loading curve and NIKE3D calculates and outputs the appropriate loading curve necessary to meet the strain rate constraint. This load curve can then be used by the machinist when forming the part. Details of the load scheduler implementation are provided in this report along with examples of its application.

Typically superplastically formed parts are very thin and the majority of their deformation is due to membrane deformation as opposed to bending. This allows the use of membrane type elements to model the parts. Because membrane elements only require

twelve degrees of freedom as opposed to twenty four for the shell element , they are much more efficient and require far less storage so that larger parts and finer meshes can be modeled. As part of the effort to simulate the SPF process, a membrane element was implemented into NIKE3D. The implementation is described in the following along with an example of its application.

LOAD SCHEDULER

The finite element discretized equations of motion provide the following coupled set of equations to be solved,

$$M\ddot{u} + f^{int}(u,t) = f^{ext}(t) \tag{1}$$

where u is the vector of displacements, M is the mass matrix, f^{int} is the vector of internal forces calculated for the stresses, and f^{ext} is the vector of externally applied loads. Typically Eq. (1) is solved on a step by step basis such that the solution u_n is known at time t_n and the solution u_{n+1} at time t_{n+1} is to be calculated in Eq. (2) via the Newton or quasi Newton Raphson methods.

$$M\ddot{u}_{n+1} + f^{int}(u_{n+1}) = f^{ext}(t_{n+1}) \tag{2}$$

Usually the external force is known, but with process control the external force is an unknown which is computed to satisfy the constraint equation. For a single constraint, the external force is parameterized by the unknown scalar p such that (2) is restated.

$$M\ddot{u}_{n+1} + f^{int}(u_{n+1}) = f^{ext}(p_{n+1}, t_{n+1}) \tag{3}$$

In the NIKE3D implementation this parameter may be a pressure, applied displacement or applied force. In what follows the loading parameter p will be referred to as the pressure for brevity, but is understood to be any scalar loading parameter. The parameter p_{n+1} is chosen to maintain an average effective plastic strain rate $\dot{\varepsilon}$ at some chosen value according to the constraint Eq. (4).

$$g(u_{n+1}) = \frac{\int_{V_p} \dot{\varepsilon}_{n+1}\, dV_p}{\int_{V_p} dV_p} - \dot{\varepsilon}^{targ} = \dot{\varepsilon}^{avg}_{n+1} - \dot{\varepsilon}^{targ} = 0 \tag{4}$$

where the integration is made over the volume V_p which contains a given upper percentile of strain rates. For example, the default percentage used by NIKE3D uses the volume containing the upper 10% of strain rates $\dot{\varepsilon}$. This volume may not necessarily be continuous. The system of equations to be solved is now (3) and (4).

There are a number of different methods for process control: Grandhi et. al. (1993), Haberman et. al. (1995), Rama and Chandra (1991), and Bonet et. al. (1989). The nested secant method used to provide process control herein is similar in form to that used for 2D analysis by Engelmann et. al. (1992) but calculates the pressures differently in the initial iterations and uses a secant method augmented by a regula falsi algorithm in the later iterations.

In the nested secant method the i^{th} trial pressure p^i_{n+1} is calculated by the modified secant method (as will be described) and used in (3) to calculate u^i_{n+1} in the usual fashion. Then u^i_{n+1} is then used to calculate $\dot{\varepsilon}^{i+1}_{n+1}$ which is substituted into (4) to check whether the constraint is adequately maintained. In NIKE3D the upper and lower bounds $k_{\max}$ and $k_{\min}$ are input to determine the adequacy of the solution. If the inequality of Eq. (5) is satisfied, then p^i_{n+1} is deemed acceptable and the algorithm procedes to the $n+2$ step.

$$\kappa_{min} \le \dot{\varepsilon}^{avg}_{n+1} \le \kappa_{max} \qquad (5)$$

If (5) is not satisfied, then the $(i+1)^{th}$ trial pressure is calculated by the modified secant method and the iterations continue. From hereon $\dot{\varepsilon} = \dot{\varepsilon}^{avg}$ is used for brevity.

The algorithm used to calculate pressure iterates has three stages. Stage (i) and (ii) are secant type methods and stage (iii) uses the usual secant method augmented with the regula falsi algorithm. (Kreyszig, 1983). The algorithm is given below:

> At the beginning of time step $n+1$, p_{n-1}, p_n and u_n are known. The trial pressures p^i_{n+1} are calculated by (i)-(iii) below and provides u^i_{n+1} from (3). If (5) is satisfied then $p_{n+1} = p^i_{n+1}$, $u_{n+1} = u^i_{n+1}$ and we proceed to the next time step.

If (5) is not satisfied $p^{i+1}{}_{n+1}$ is calculated from (i)-(iii) and $u^{i+1}{}_{n+1}$ is calculated from (3).

(i) For $i = 0$, calculation of $p^0{}_{n+1}$ is based on the previous time step $\Delta t_n = t_n - t_{n-1}$ such that:

$$\frac{\Delta p}{\Delta \varepsilon} = \frac{p_n - p_{n-1}}{\dot{\varepsilon}_n \Delta t_n} \tag{6}$$

and

$$p^0_{n+1} = p_n + \frac{\Delta p}{\Delta \varepsilon} \dot{\varepsilon}^{arg} \Delta t_{n+1} = p_n + (p_{n+1} - p_n)\left(\frac{\dot{\varepsilon}^{arg}}{\dot{\varepsilon}^0_n}\right)\left(\frac{\Delta t_{n+1}}{\Delta t_n}\right) \tag{7}$$

(ii) For $i = 1$, it is assumed* that $\dot{\varepsilon}_{n+1} = 0$ would lead to $p_{n+1} = p_n$. Therefore $p^1{}_{n+1}$ is calculated:

$$p^1_{n+1} = p_n + \frac{\Delta p}{\Delta \varepsilon}\left(\dot{\varepsilon}^{arg} - 0\right) = p_n + \frac{p^0_{n+1} - p_n}{\dot{\varepsilon}^0_{n+1}} \dot{\varepsilon}^{arg} \tag{8}$$

(iii) For $i > 1$, the recursion (9) is used:

$$p^i_{n+1} = p_a + \frac{p_a - p_b}{\dot{\varepsilon}_a - \dot{\varepsilon}_b}\left(\dot{\varepsilon}^{arg} - \dot{\varepsilon}_a\right) \tag{9}$$

For $i = 2$ $\dot{\varepsilon}_a = \dot{\varepsilon}^2_{n+1}$, $\dot{\varepsilon}_b = \dot{\varepsilon}^1_{n+1}$, $p_a = p^1{}_{n+1}$ and $p_b = p^0{}_{n+1}$.

For $i > 2$ values of $\dot{\varepsilon}_a$ and $\dot{\varepsilon}_b$ in (9) are determined as follows:

When $\left(\dot{\varepsilon}^{arg} - \dot{\varepsilon}^i_{n+1}\right) \cdot \left(\dot{\varepsilon}^{arg} - \dot{\varepsilon}_a\right) > 0$ occurs, the secant method is used such that:

$$\begin{aligned} \dot{\varepsilon}_a &= \dot{\varepsilon}^i_{n+1},\ \dot{\varepsilon}_b = \dot{\varepsilon}_a \\ p_a &= p^i_{n+1},\ p_b = p_a \end{aligned} \tag{10}$$

---

* This assumption is not true when there is softening and the pressure load actually needs to unload to maintain a given strain rate. Excessive thinning of a sheet occurring during a deep draw can yield such softening. Nevertheless, the algorithm will solve the problem at the expense of extra pressure iterations.

When $\left(\dot{\varepsilon}^{targ} - \dot{\varepsilon}^{i}_{n+1}\right) \cdot \left(\dot{\varepsilon}^{targ} - \dot{\varepsilon}_{a}\right) < 0$ occurs, the method switches to regula falsi for the remaining pressure iterations to trap the desired strain rate. Thereon:

$$\text{If } \left(\dot{\varepsilon}^{targ} - \dot{\varepsilon}^{i}_{n+1}\right) \cdot \left(\dot{\varepsilon}^{targ} - \dot{\varepsilon}_{a}\right) < 0 \quad \text{then} \quad \begin{array}{l} \dot{\varepsilon}_{a} = \dot{\varepsilon}^{i}_{n+1},\ \dot{\varepsilon}_{b} = \dot{\varepsilon}_{a} \\ p_{a} = p^{i}_{n+1},\ p_{b} = p_{a} \end{array} \tag{11}$$

$$\text{If } \left(\dot{\varepsilon}^{targ} - \dot{\varepsilon}^{i}_{n+1}\right) \cdot \left(\dot{\varepsilon}^{targ} - \dot{\varepsilon}_{a}\right) > 0 \quad \text{then} \quad \begin{array}{l} \dot{\varepsilon}_{a} = \dot{\varepsilon}^{i}_{n+1},\ \dot{\varepsilon}_{b} = \dot{\varepsilon}_{b} \\ p_{a} = p^{i}_{n+1},\ p_{b} = p_{b} \end{array} \tag{12}$$

The nested secant iterations can be considered an implicit method since multiple iterations are used to calculate the pressure to some error tolerance (5). Nevertheless the above algorithm may be used as an explicit method by setting the bounds in (5) very high. By doing this only step (i) is performed in the above algorithm such that the pressure is scaled by (7). In order to get good results from any explicit algorithm small time steps must be used. The implicit algorithm allows much larger time steps to be taken with more control of the results.

The above algorithm works well with the auto time steppers available in NIKE3D. The pressure iterations loop is nested within the auto time stepper loop. If at any time within the pressure iterations the equilibrium iterations used to satisfy (3) fail, the time step is cut and the pressure iterations begin with a new Δt_{n+1}.

The regula falsi method given by (9), (11) and (12) can sometimes provide better convergence by "trapping the pressure." Use of the secant method alone (Eqs. (9) and (10)) on particular problems sometimes never converge. Use of the regula falsi on these problems found that two pressures arbitrarily (i.e. $\Delta p / p = 1 \times 10^{-6}$) close together would provide two different strain rates that would not fall within the inequality (5). This apparent (possibly numerical) bifurcation probably occurs due to the fact that the softening effect due to thinning offsets the stiffening effect due to strain rate hardening. When NIKE3D enters the regula falsi algorithm it checks the relative pressure difference

to see if this "bifurcation" has occurred. If $\Delta p / p < 1 \times 10^{-4}$, then the time step is decreased and the pressure iterations restarted.

MEMBRANE ELEMENT

Often parts formed by SPF are very thin such that most of the deformation that occurs during forming is membrane as opposed to bending. This warrants the use of membrane elements which can provide a significant computational savings over shell elements. This is particularly important for implicit analysis with process control because of the additional iterations needed to solve the constraint equations.

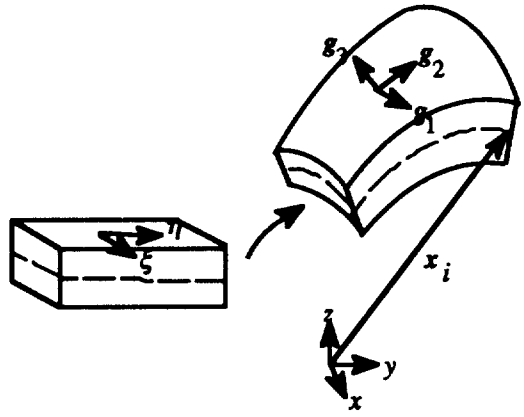

Fig. (1) Two parameter representation of membrane element

A large strain four node membrane element was developed for NIKE3D. The finite element formulation is based on the following two parameter (ξ, η) description of the membrane element kinematics (c.f. Fig. 1).

$$\boldsymbol{x} = \sum_{i=1}^{4} N_i(\xi,\eta)\ \boldsymbol{x}_i \tag{11}$$

where $\boldsymbol{x}$ is the vector locating the midsurface of the membrane, (ξ, η) is the local coordinates and $\boldsymbol{x}_i$ is the vector locating the i^{th} node. The covariant basis for the membrane element is given by

$$\boldsymbol{g}_1 = \frac{\partial \boldsymbol{x}}{\partial \xi} \qquad \boldsymbol{g}_2 = \frac{\partial \boldsymbol{x}}{\partial \eta} \qquad \boldsymbol{g}_3 = \frac{\partial \boldsymbol{x}}{\partial \xi} \times \frac{\partial \boldsymbol{x}}{\partial \eta} \tag{12}$$

The lamina coordinate system is a Cartesian coordinate system constructed from the convected coordinate system as such (Hughes and Liu, 1983):

$$e_1^\ell = g_1 / \|g_1\| \qquad e_2^\ell = g_1 \times g_2 / \|g_1 \times g_2\| \qquad e_3^\ell = g_3 / \|g_3\| \tag{13}$$

The velocity gradient (14) is calculated from (11) and (12) as such,

$$L = \frac{\partial \dot{x}}{\partial x} = \frac{\partial \dot{x}}{\partial \xi} \frac{\partial \xi}{\partial x} \quad \text{where } \xi = (\xi, \eta) \tag{14}$$

The following describes the numerical implementation,

(i.) Using the Jaumman rate as the objective stress rate, the stress in the global coordinate system at t_n is half rotated to the midpoint configuration $t_{n+1/2}$ via the Hughes Winget integration of the spin given by the anti-symetric part of (14).

(ii.) The midpoint stress from (i.) is then rotated to the midpoint $t_{n+1/2}$ lamina coordinate system using Eq. (13).

(iii.) The rate of deformation gradient calculated from the symmetric portion of (14) is rotated to the lamina coordinate system (13) at the midpoint configuration and the rotated stresses from (ii.) are updated by the constitutive law.

(iv.) The through thickness strain given by $d_{33}^\ell = e_3^\ell \cdot L \cdot e_3^\ell$ is zero, a value of d_{33}^ℓ is calculated to provide a zero out of plane stress. This strain is then used to calculate the change in thickness of the membrane.

(v.) The stresses in (iii.) are rotated back down to the global coordinate system.

(v.) Another half rotation as in (i.) is then applied to update the stress in (v.).

The above scheme is analogous to the shell element stress update algorithms given by the Hughes Liu element (Hughes and Liu, 1983). In the membrane element, stress is only calculated at the midsurface such that no through thickness integration is made. Furthermore, no fiber directions (Hughes and Liu, 1983) or director vectors (Simo and Fox, 1987) are include in (11) such that rotational degrees of freedom are not necessary. This makes the membrane element much more efficient than the shell element since it has only twelve degrees of freedom as opposed to twenty-four for the shells in NIKE3D.

Since the membrane elements have no bending stiffness, it is necessary to pretension them. The element geometric stiffness then provides the necessary stability to the global stiffness matrix. The ability to apply a biaxial pretension to shells and membranes was added to NIKE3D to accommodate the new membrane element.

Example Applications

The following are examples of SPF applications of the load scheduler and membrane elements in NIKE3D. In both examples, material model 19 (Strain Rate Plasticity) was used to model the sheets being formed.

The first example (Fig. 2) is an application of the load scheduler controlling the displacement of a die during a stamp forming. Quite often it is desired to use displacement control as opposed to force control when possible due to the added stability. The upper and lower dies are rigid and the sheet is composed of shell elements. The desired strain rate was $2x10^{-4}$ /sec. and the lower and upper bound tolerances were given by $1.9x10^{-4}$ and $2.1x10^{-4}$. Displacement and average strain rates vs. time are shown in Figs. 3 and 4. The strain rate drops at the last step when the sheet is finally pressed into the bottom die.

Figs. 5 and 6 show an example of the process used to form SPF "packs" into panels such as a skin panel used in aerospace structures. A pack is a layer of sheets which are welded together along lines to form a specified pattern. Gas is then blown in between the sheets. As the pressure of the gas builds, the constraint of the welds causes the sheet to form "pillows" which are blown up into a die cover to form the part. Typically these parts are more complex than the one shown in Figs. 5 and 6 such that they may contain many irregular shaped pillows. Rigid shells where used to model the die. The membrane elements describe above were used to model the sheet since the sheet is very thin and the membranes are much more efficient than shells. The pressure schedule and resulting strain rates are shown in Figs. 7 and 8. The desired strain rate was $2x10^{-4}$ /sec. and the lower and

upper bound tolerances were given by $1.6x10^{-4}$ and $2.2x10^{-4}$. In NIKE3D, the load scheduler is given an activation time at which it begins maintaining strain rate constraints. The activation time was 800 s. in this example as seen from Fig. 8. The large strain rate threshold and small time steps used caused the pressure scheduler to work almost explicitly such that it only needed to iterate on the pressure 5 times during the 51 time steps.

References

Bonet, J., H.S. Wargadpura and R.D. Wood, "A Pressure Cycle Control Algorithm for Superplastic Forming," *Communications in Applied Numerical Methods*, Vol. 5, **1983**.

Engelemann, B.E., R. Whirley and P. Raboin, "Adaptive Superplastic Forming Using NIKE2D with ISLAND," University of California, Lawrence Livermore National Laboratory, Rept., UCRL-JC-111228, **1992**.

Hughes, T.J.R, and W.K. Liu, "Nonlinear Finite Element Analysis of Shells: Part I-Three dimensional Shell," *Computer Methods in Applied Mechanics in Engineering*, Vol. 15, No 9, **1981**.

Kreyszig, E., Advanced Engineering Mathematics, Wiley, New York, **1983**.

Grandhi, R., Anand Kumar, Anil Chaudhary and James Malas, "State-Space Representation of Non-linear Material Deformation Using the Finite Element Method," *Int. J. Num. Meth. Eng.*, Vol. 36, **1993**.

Maker, B.N., "NIKE3D: An Implicit, Finite-Deformation, Finite Element Code for Analyzing the Static and Dynamic Response of Three Dimensional Solids," University of California, Lawrence Livermore National Laboratory, Rept., UCRL-MA-105268, Rev. 1, **1995**.

Rama, S.C., and N. Chandra, "Development of a Pressure Prediction Method for Superplastic Forming Processes," *International Journal of Nonlinear Mechanics*, Vol. 26, No. 5, **1991**.

Simo, J.C., and D.D. Fox, "On a Stress Resultant Geometrically Exact Shell Model. Part I: Formulation and Optimal Parameterization," *Computer Methods in Applied Mechanics and Engineering*, Vol. 72, **1989**.

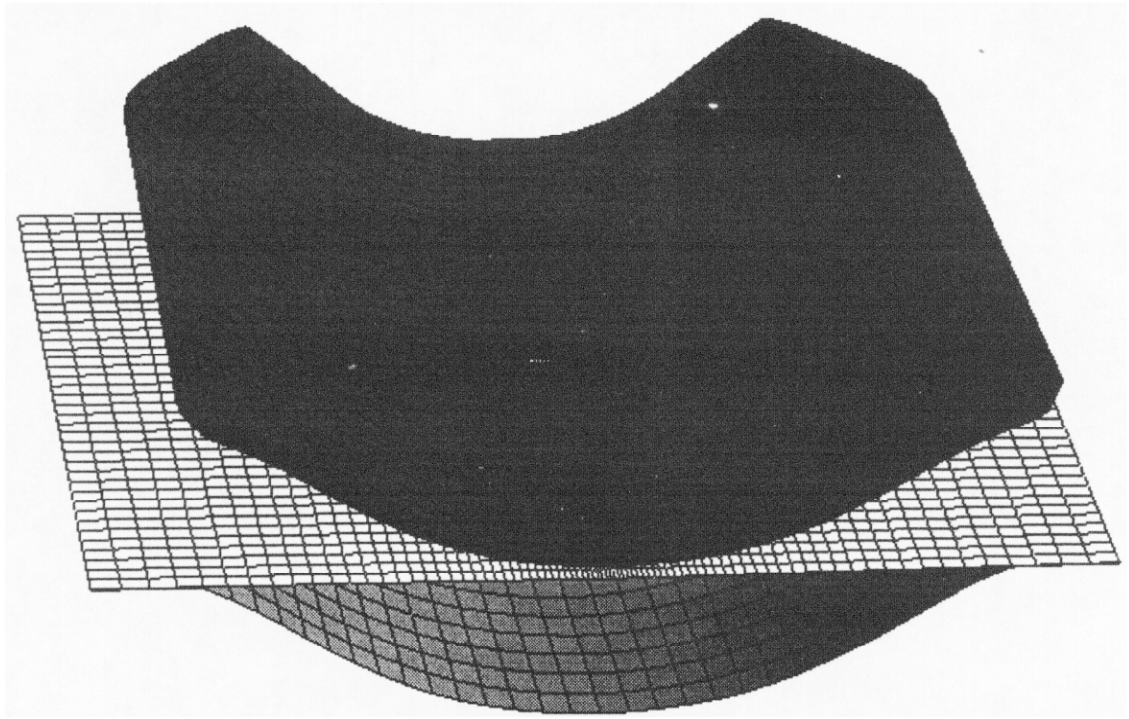

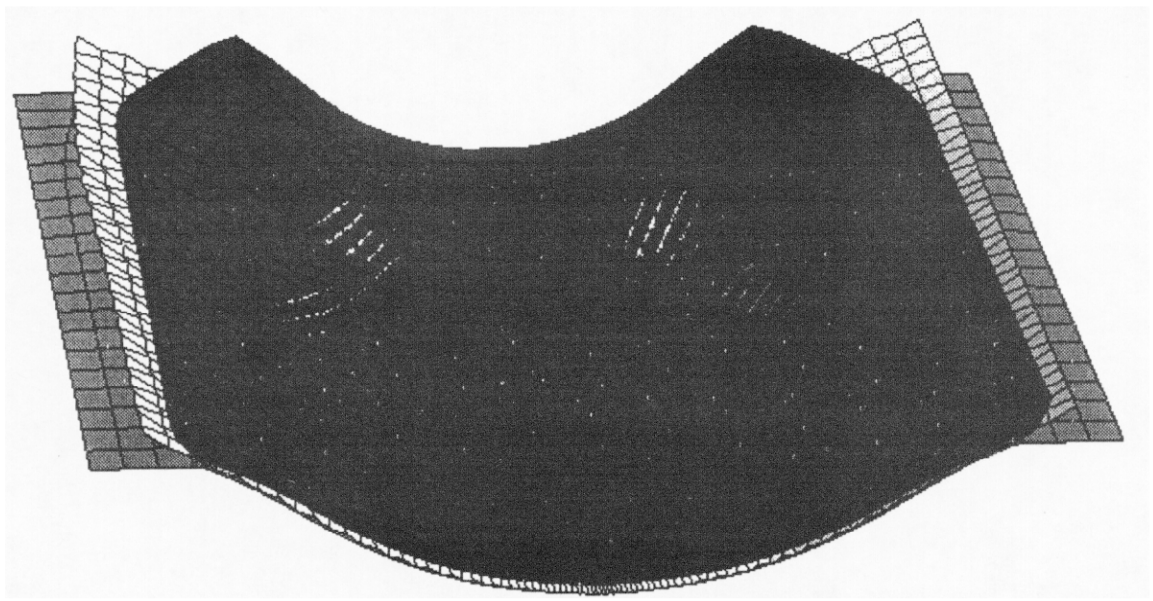

Fig. 2. Forming of sheet with displacement controlled by load scheduler.

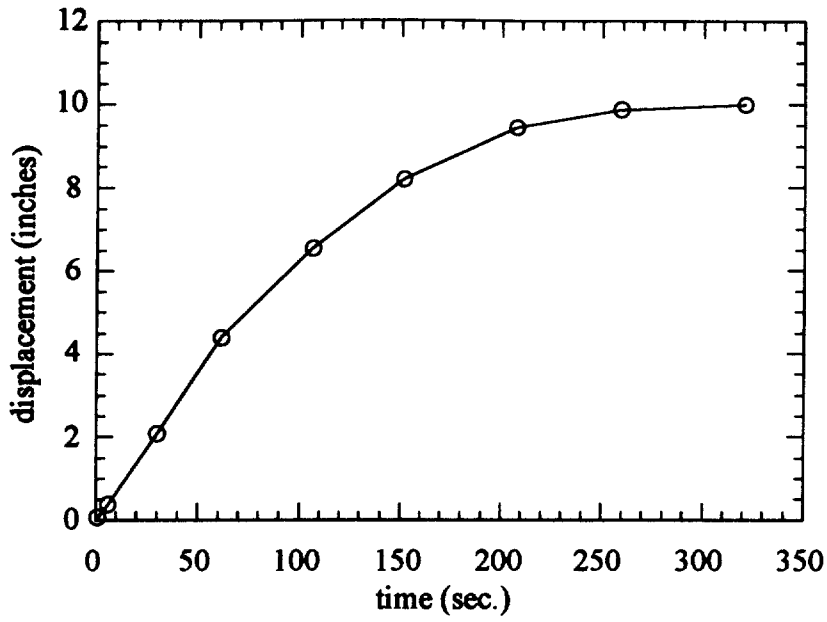

Fig. 3. The displacement vs. time of the upper die as prescribed by the load scheduler.

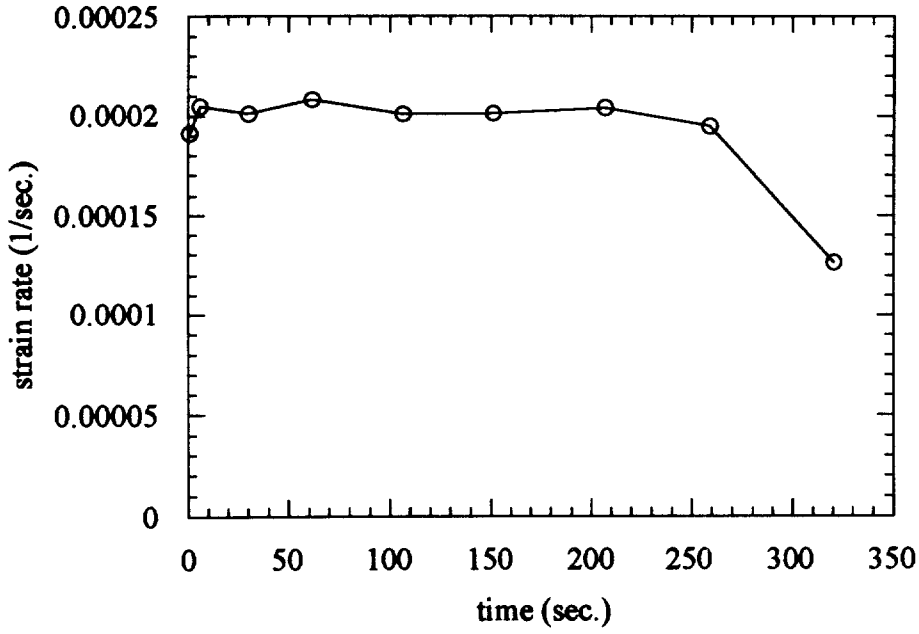

Fig. 4. The resulting strain rate vs. time for the stamp forming.

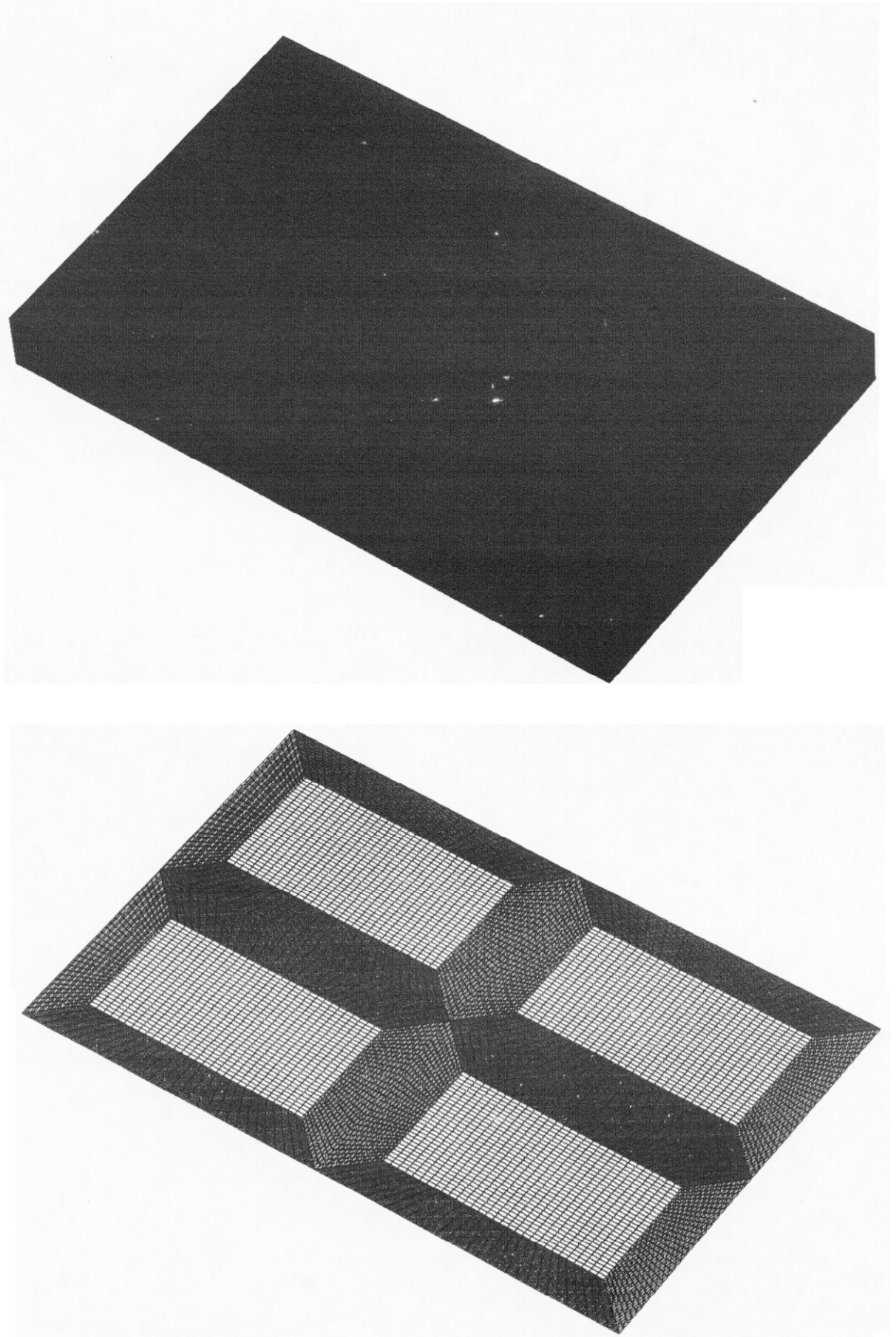

Fig. 5. SPF pack. Upper die shown above. Sheet shown below. Only the top sheet need be modeled from symmetry. The welds are modeled by fixed displacement boundary conditions which divide the sheet into four sections.

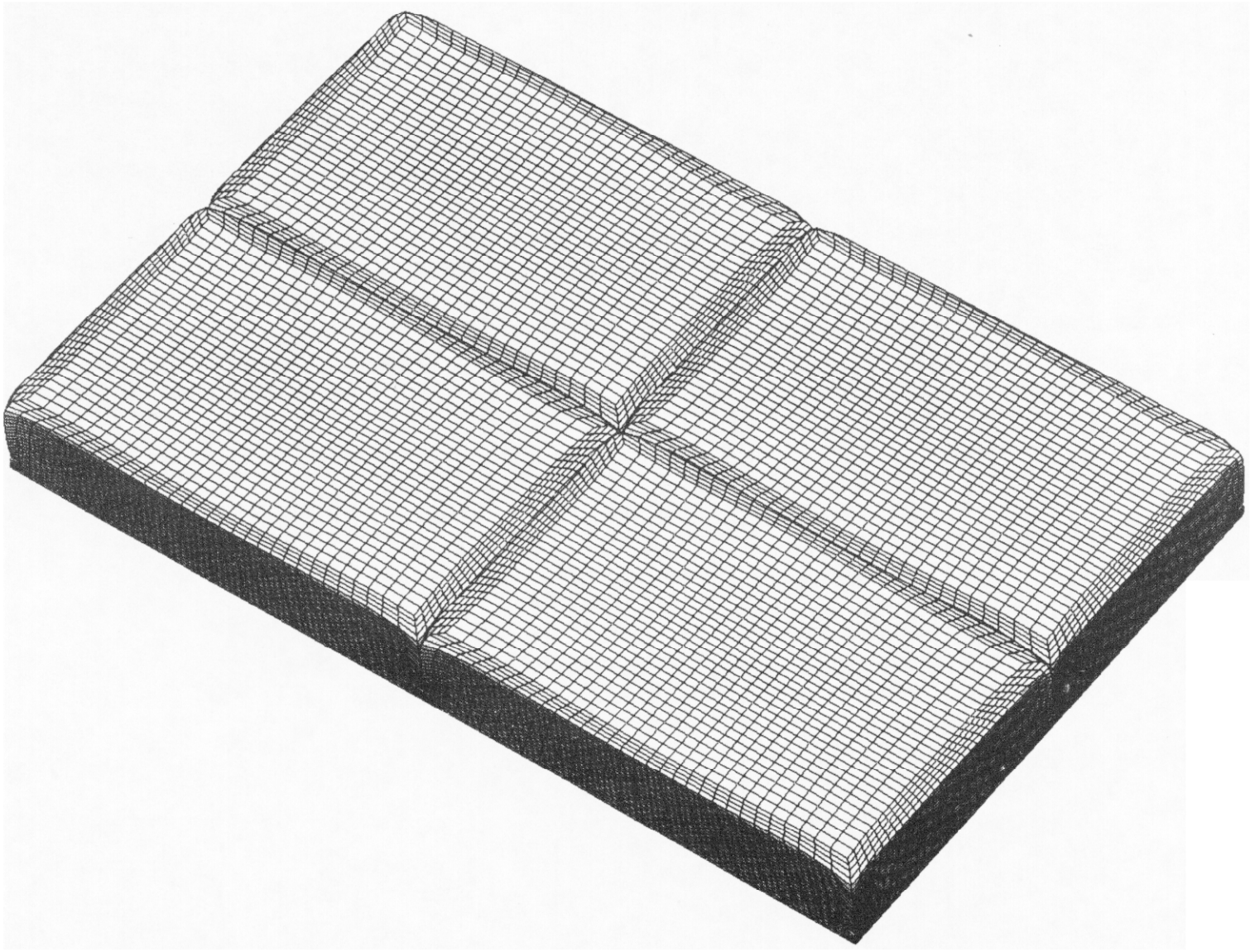

Fig. 6. Top half of formed panel.

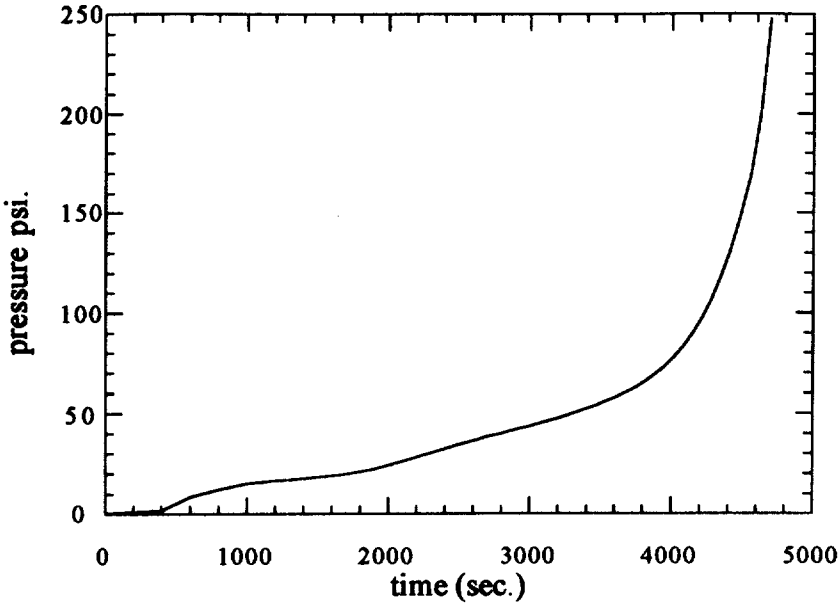

Fig. 7. Pressure vs. time curve provided by load scheduler for forming SPF panel.

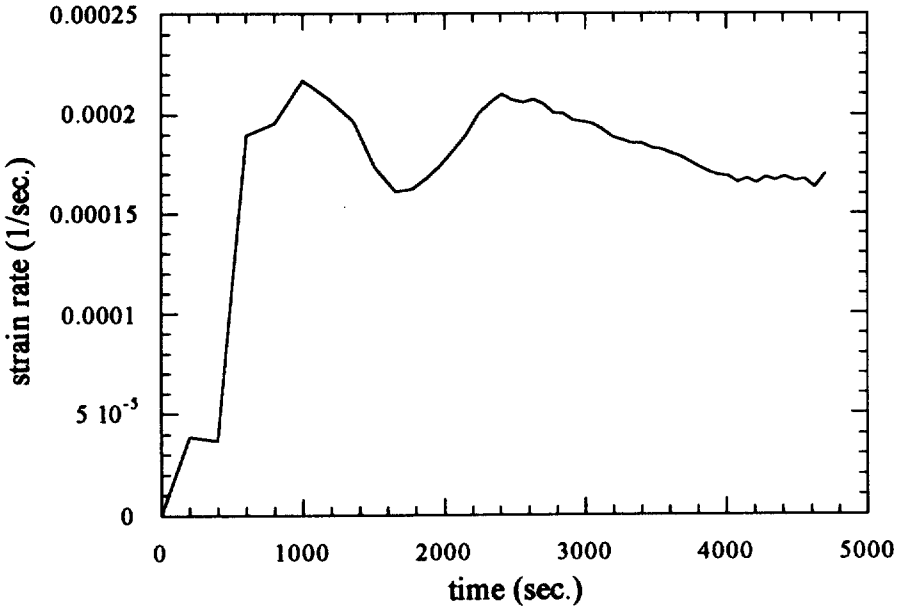

Fig. 8 Resulting strain rate using pressure scheduler when forming SPF panel.

Technical Information Department • **Lawrence Livermore National Laboratory**
University of California • Livermore, California 94551